

PAPER

High- T_c Cooper-pair injection in a semiconductor–superconductor structure

To cite this article: Shlomi Bouscher *et al* 2020 *J. Phys.: Condens. Matter* **32** 475502

View the [article online](#) for updates and enhancements.

You may also like

- [Magnetotransport in graphene nanoribbons sandwiched by superconductors at side edges](#)
Y Takagaki
- [Andreev reflection of massive pseudospin-1 fermions](#)
W Zeng and R Shen
- [Andreev reflection without Fermi surface alignment in high- \$T_c\$ van der Waals heterostructures](#)
Parisa Zareapour, Alex Hayat, Shu Yang F Zhao *et al.*






IOP | ebooks™

Bringing together innovative digital publishing with leading authors from the global scientific community.

Start exploring the collection—download the first chapter of every title for free.

High- T_c Cooper-pair injection in a semiconductor–superconductor structure

Shlomi Bouscher^{1,3} , Zhixin Kang^{2,3}, Krishna Balasubramanian¹ ,
Dmitry Panna¹, Pu Yu², Xi Chen² and Alex Hayat^{1,3} 

¹ Department of Electrical Engineering, Technion, Haifa 32000, Israel

² State Key Laboratory of Low Dimensional Quantum Physics and Department of Physics, Tsinghua University, Beijing, 100084, People's Republic of China

E-mail: alex.hayat@ee.technion.ac.il

Received 1 March 2020, revised 30 July 2020

Accepted for publication 11 August 2020

Published 27 August 2020



Abstract

We observe Andreev reflection in a YBCO–GaN junction through differential conductance spectroscopy. A strong characteristic zero-bias peak was observed and persisted up to the critical temperature of the superconductor with a smaller superconducting order parameter $\Delta \sim 1$ meV. The presence of Andreev reflection with the small Δ in comparison to its value for high- T_c superconductors forms an important milestone toward demonstration of superconducting proximity in high- T_c /semiconductor junctions. Experimental results were then compared to the theoretical model with good agreement. Efficient injection of Cooper pairs into direct bandgap semiconducting structures, together with high transition temperature of YBCO, can pave the way to novel optoelectronics and quantum optical studies of high- T_c materials.

Keywords: high- T_c superconductivity, superconductor–semiconductor, Andreev reflection

(Some figures may appear in colour only in the online journal)

Hybrid superconductor–semiconductor structures form a rapidly growing field of research [1, 2], which utilizes the unique physical properties of the superconducting state [3] along with the vast knowledge and fabrication capabilities in the field of semiconductors. Various applications involving such hybrid structures have been shown, including superconducting light-emitting diodes (SLEDs) and quantum dots [4–6], Bell-state analyzers [7] and superconductor-based waveguide amplifiers [8]. Of note is the SLED which is a hybrid superconductor–semiconductor device, where superconducting Cooper pairs recombine with semiconductor hole pairs, forming polarization-entangled photon pairs [9]. While low- T_c Cooper-pair injection into semiconductors has been observed previously [10–13], including the recent demonstration of radiative recombination of Cooper pairs in SLED devices [14], they must operate at very low temperatures due

to low critical temperature of the superconductor being used (~ 10 K).

High- T_c superconductors have the strong advantage of having a high critical temperature (above the boiling temperature of liquid nitrogen of 77 K). Realization of high- T_c superconductor–semiconductor light-emitting structures can allow using quantum optics to probe high- T_c superconductors. Although there has been an unprecedented effort to understand the mechanism of high- T_c superconductivity, it still remains unsolved. This difficulty stems largely from the fact that even in the normal state above T_c , these materials are not well-understood. Superconductivity is obtained by impurity doping, and the parent material is an antiferromagnetic strongly-correlated Mott insulator [15], where single-particle band theory description fails. Recent studies have revealed a complex phase diagram vs temperature and doping, as well as the unconventional d-wave symmetry of the order parameter in high- T_c materials [16, 17]. Other aspects are still being debated—such as the appearance of self-organization with non-uniform charge carrier density (stripes) [18], and the origin of the pseudogap phase [19, 20] with possible relation

³ Authors to whom any correspondence should be addressed.

⁴ Both authors contributed equally to this work.

to the formation of Cooper pairs without condensation above T_c . Various experimental techniques have been employed to study unconventional superconductivity—ranging from electrical transport and tunneling [21–28] to infrared electrodynamics [16], resulting in a substantial body of knowledge. However, these techniques do not have access to the phase information of individual charge carriers, or various correlations within the Cooper pairs such as classical spin and momentum correlations, as well as quantum entanglement. Optical access to individual charge carriers through quantum light–matter interaction with relative phase information and quantum correlations can provide important insights into the nature of unconventional superconductivity and pave the way for novel optoelectronics.

The challenge in using high- T_c superconductors is that their growth and fabrication poses a greater challenge in comparison to their low- T_c counterparts [29]. High- T_c superconductors require stringent growth conditions and can degrade rapidly when incorporated into a given semiconductor device or even under standard ambient conditions [30, 31]. Nevertheless, devices incorporating high- T_c superconductors have been successfully demonstrated. These include terahertz sources [32], RF SQUIDs [33] and YBCO–Graphene junctions [34] to name a few. In addition, much research has been done on Andreev bound states in high- T_c superconductors [24–28].

The second required component for the high- T_c superconductor–semiconductor junction is a semiconductor such as GaN which has a decomposition temperature of 1300 K [35], a property enabling it to serve as the growth substrate for YBCO at high temperatures [36, 37]. Epitaxial growth of YBCO on GaN was demonstrated recently, however no Cooper pair injection was achieved [38].

Here we demonstrate high- T_c Cooper-pair injection in a superconductor–semiconductor junction (YBCO–GaN), exhibiting strong Andreev reflection in the electrical conductance spectra. High injection efficiency was achieved by improving the semiconductor–superconductor interface and optimizing the YBCO growth process. The combination of YBCO with a GaN-based LED structure allows for the design of high-temperature SLEDs. A model for describing the electrical conductance of high- T_c superconductor–semiconductor junctions [39] was then used in good agreement with our experimental observations.

For our experiments, a 3.5 μm thick n -GaN layer ($n \sim 5 \times 10^{18} \text{ cm}^{-3}$) with the top 200 nm thick heavily doped ($\sim 2 \times 10^{19} \text{ cm}^{-3}$) was initially grown on buffered Al_2O_3 substrate. A 100 nm YBCO layer was then grown in a suitable high vacuum chamber using a customized pulsed laser deposition system [40]. A KrF excimer laser (248 nm) with pulse energy of 38 mJ and a repetition rate of 2 Hz was used. The sample was heated up to a temperature of 650 $^\circ\text{C}$ at a rate of 18 $^\circ\text{C min}^{-1}$ and was kept under oxygen pressure of 0.195 mbar for the duration of the growth. After growth was completed, that sample was cooled down at a rate of 18 $^\circ\text{C min}^{-1}$ in a 100 mbar oxygen atmosphere to avoid the formation of oxygen vacancies.

For characterization an XRD test was performed (figure 1(c)) to check for the composition of the various layers. The obtained XRD profile matched the XRD profile

from the previous work with the same characteristic peaks indicating a layer stack composed of YBCO, GaN and a Sapphire substrate. Additional characterization was performed using SEM (figures 1(a) and (b)) where a portion of the sample was etched using a focused ion beam. The test revealed a top YBCO layer with 100 nm thickness. Below the YBCO layer was a 3.5 μm GaN layer followed by the sapphire substrate.

Following the growth of multiple samples, half of each sample was dipped in a solution of 0.01% H_3PO_4 in order to remove the top YBCO layer and expose the bottom GaN layer. The samples were then placed inside a ceramic chip holder (LCC28) with aluminum wires being bonded to both YBCO and GaN layers via wedge bonding. The samples were then inserted into the cryostat for testing.

The measurement of temperature dependent resistance has revealed a critical temperature of about ~ 80 K which is close to the maximum reported value of 93 K for YBCO [41]. Residual series resistance of $\sim 120 \Omega$ below T_c was also observed and is attributed to non-superconducting regions of the device. The wide transition between the normal and superconducting state (figure 2(b)) can be attributed to multiple domains inside the superconductor having different critical temperatures. Thus, true global superconductivity is obtained at a lower (albeit still high) temperature (~ 80 K) in comparison to an ordered superconductor. Since YBCO/GaN growth was first demonstrated very recently [38] the growth process may not be fully optimized; however, important information can be extracted from our measurements. Both the broadening and reduced T_c can be attributed to large defect density and diffusion of Ga atoms from the GaN layers into the YBCO [38]. As the exact profile of the diffused Ga atoms is unknown, we cannot pinpoint the exact location inside the junction where Andreev reflection takes place. Electrical transport measurements were then conducted using four-probe configuration (figure 2(a)). This configuration ensures that only the sample resistance is measured and not the wires or the sample-wire interface. This is due to the fact that the only measured voltage is the voltage drop on the device itself. Thus even if Andreev reflection does take place between the YBCO and the aluminum bonding wires, it will not appear in our measurement. The conductance measurements (figure 3) revealed a strong zero-bias peak with significant dependence on the temperature of the junction. The peak conductance decreases as the temperature increases up to the critical temperature. The width of the zero-bias peak increases with increasing temperature due to the growing thermal energy of the charge carriers, which broadens the peak.

In order to model the experimental results we used a theoretical description of carrier injection and the resulting conductance spectra of high- T_c superconductor–semiconductor junctions formulated by Tanaka and Kashiwaya [39]. The model is based on the Blonder–Tinkham–Klapwijk (BTK) theory [42] describing the behavior of quasiparticle excitations from the superconducting state. Using the quasiparticle description, the electrical conductance spectra can be calculated. The complete wave function is composed of two

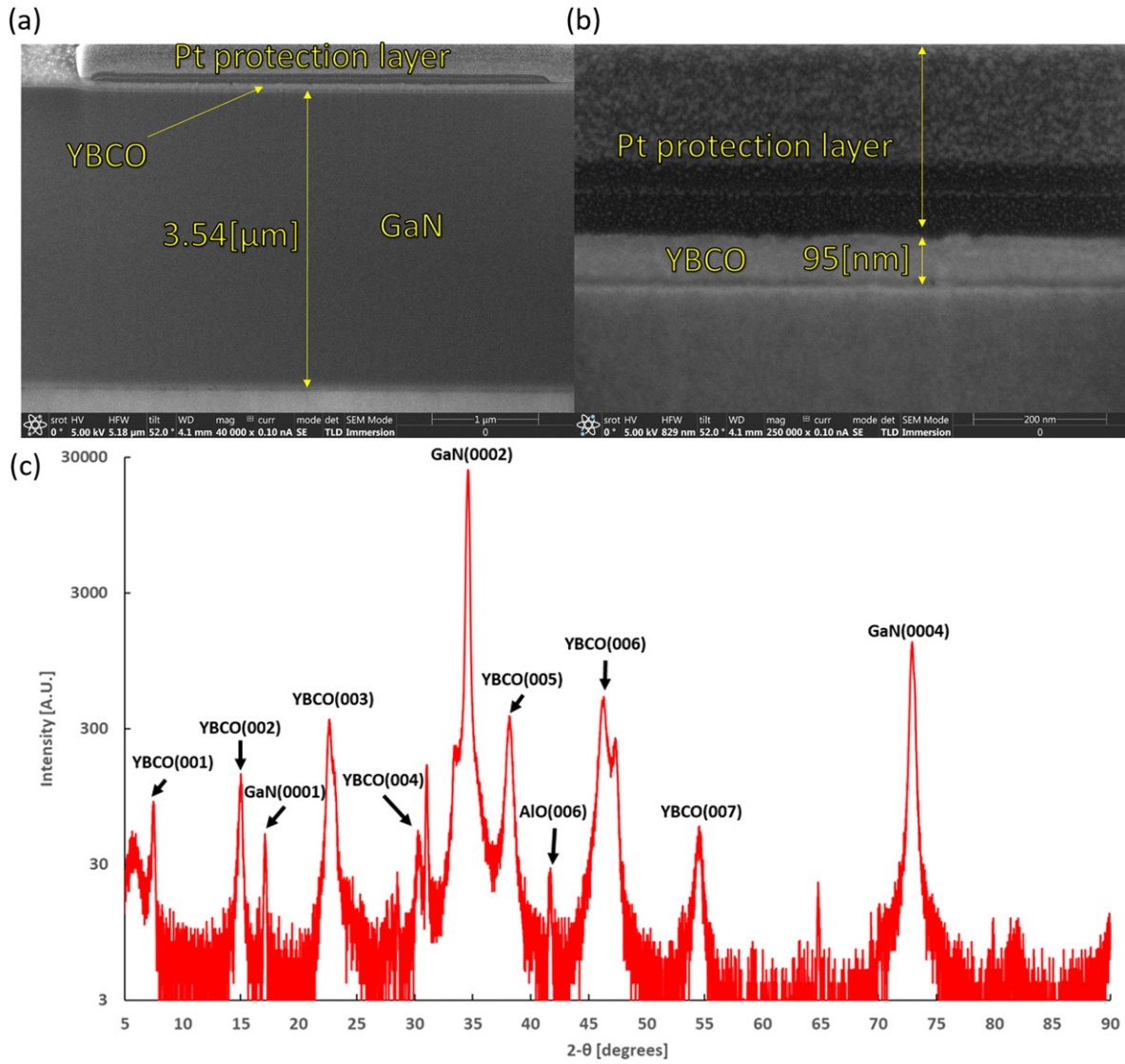


Figure 1. (a) and (b) SEM images of the entire device stack showing a 3.5 μm GaN layer with a thin YBCO layer on top. The Pt protection layer was added during SEM imaging. (c) XRD peak spectrum of the measured sample. Characteristic peaks to YBCO, GaN and sapphire (AlO) were measured.

components, satisfying the Bogoliubov–de-Gennes equations:

$$\begin{cases} \left[-\frac{\hbar^2}{2m} \frac{d^2}{dx^2} - \mu(x) + V(x) \right] \cdot u(x) + \Delta(x) \cdot v(x) = E \cdot u(x) \\ -\left[-\frac{\hbar^2}{2m} \frac{d^2}{dx^2} - \mu(x) + V(x) \right] \cdot v(x) + \Delta(x) \cdot u(x) = E \cdot v(x) \end{cases} \quad (1)$$

With $\mu(x)$, $V(x)$, $\Delta(x)$ being the chemical potential, potential barrier and the superconducting order parameter correspondingly, and $u(x)$, $v(x)$ being the quasiparticle wave functions. A delta barrier is assumed to exist at the superconductor–semiconductor interface having an effective barrier strength parameter $Z = H/\hbar v_f$ where v_f is the Fermi velocity and H is the height of the delta barrier. For a small Z , the junction is transparent and Andreev reflection takes place, while for a large Z Andreev reflection is inhibited and the tunneling regime takes place. While the original BTK model copes

with superconductors described by the BCS model, YBCO is a not a BCS superconductor and thus the anisotropic model [39] is required. This model takes into account the k dependence of the superconducting order parameter Δ . If an s-wave superconductor is assumed, equations of the model reduce to the original BTK model equations. Since we included a broadening term in our model, the results for either d-wave or s-wave models result in similar spectra. The normal junction conductivity is expressed as $\sigma_N \triangleq \frac{4\lambda}{(1+\lambda)^2 + 4Z^2}$ where λ is the wave-vector mismatch between the superconductor and semiconductor. The resulting normalized conductance is:

$$\sigma_R = \frac{1 + \sigma_N |\Gamma_+|^2 + (\sigma_N - 1) |\Gamma_+ \Gamma_-|^2}{|1 + (\sigma_N - 1) \Gamma_+ \Gamma_- \exp(i[\varphi_- - \varphi_+])|^2}, \quad (2)$$

where $\Gamma_{\pm} = \frac{E - \Omega_{\pm}}{|\Delta_{\pm}|}$, $\Omega_{\pm} = \sqrt{E^2 - |\Delta_{\pm}|^2}$ and Δ_{\pm} is the pair

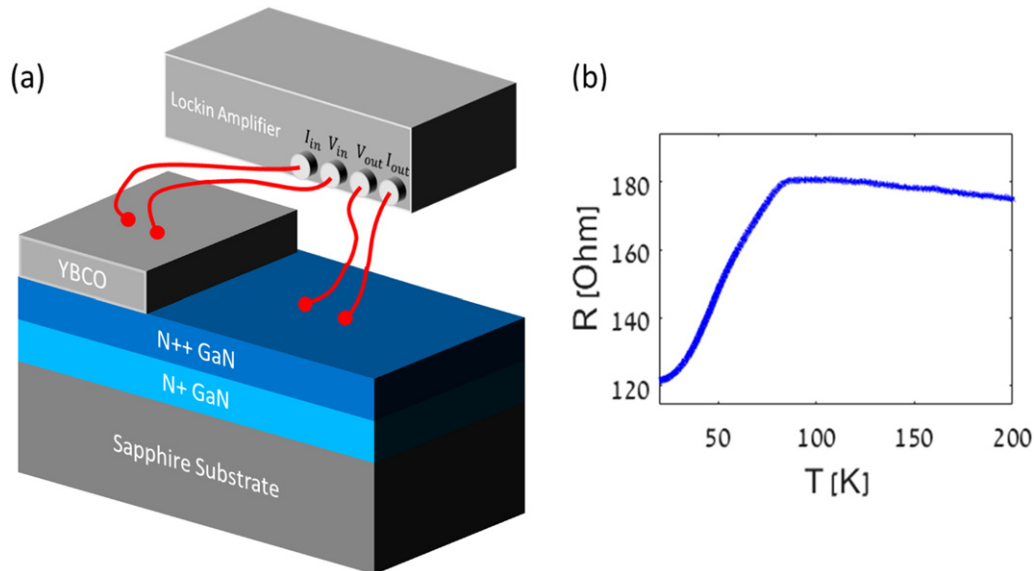


Figure 2. (a) Schematics of the device and four-probe measuring technique. (b) Measured sample resistance as function of temperature also done in a four-probe configuration (all four probes connected to the YBCO layer). Residual series resistance of non-superconducting YBCO was also observed.

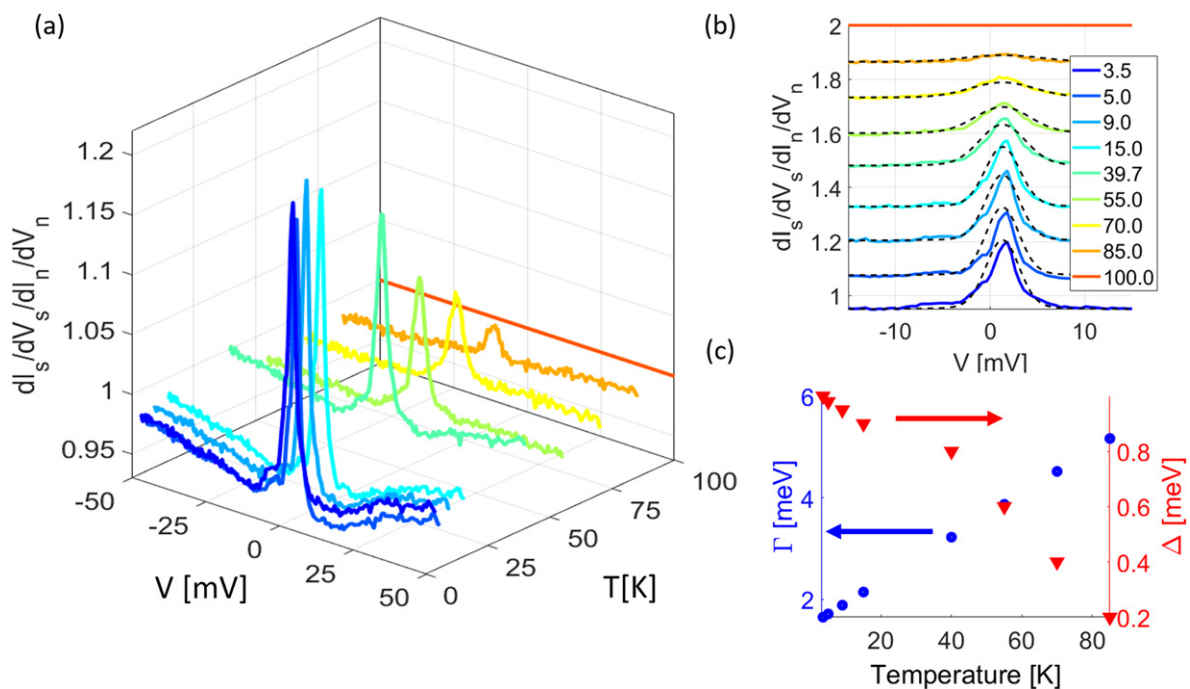


Figure 3. (a) Normalized conductance spectra of the YBCO–GaN junction. A strong zero-bias peak is evident, decreasing in magnitude and broadening up to the critical temperature. (b) Measured (solid lines) and modeled (dashed lines) spectral shapes of the zero-bias peak. (c) Extracted dependence on the temperature of the order parameter $\Delta(T)$ and broadening $\Gamma(T)$.

potential of the electron-like and hole-like quasiparticles and φ_{\pm} is the phase of each pair potential.

Using this model, a good agreement with theory was obtained (figure 3(b)) with an effective barrier strength Z of ~ 0.4 and an induced superconducting order parameter Δ of ~ 1 meV. The small value obtained for the order parameter may be attributed to the proximity effect, as superconductivity is induced in the semiconductor albeit with a reduced magnitude of the order parameter Δ (in relation to its value

in the parent superconductor) [43]. Earlier works [13] have also demonstrated similar behavior in Nb/Si junctions, with a reduced value of Δ . Moreover, disorder in the superconductor can also lead to a reduction in the value of Δ [44]. Such disorder can also be the cause behind the broadened transition in the resistance-temperature dependence (figure 2(b)). We have performed a fit for the superconducting gap Δ as well as the broadening term Γ . We have used the general form $\Gamma = \Gamma_0 + \alpha k_B T$ where Γ_0, α are fitting coefficients, k_B is the Boltzmann

coefficient and T is the sample temperature. The obtained coefficients were $\Gamma_0 = 1.5$ [meV], $\alpha = 1/2$. For Δ , a general fitting was performed with ($T = 3.5$ K) ≈ 1 [meV]. The normalized values of $\Gamma(T)$, $\Delta(T)$ (relative to 3.5 K) appear in figure 3(c). The low effective barrier strength coupled with the strong signature of Andreev reflection show that YBCO–GaN junctions can potentially have excellent electrical properties.

In conclusion, we have demonstrated strong Andreev reflection in a YBCO–GaN junction. Theoretical modeling resulted in good agreement with experimental results. The reduced value of Δ may be attributed to the superconducting proximity effect, which is strongly related to the phenomenon of Andreev reflection. This was achieved through the high doping of the GaN layer as well as a good contact between the YBCO and GaN layers. This demonstration of a high- T_c superconductor coupled to a wide-bandgap semiconductor can pave the way for future hybrid optoelectronic devices, working at higher temperatures around 100 K and enabling quantum optical probing of high- T_c superconductivity.

Acknowledgments

We would like to thank the Technion RBNI FIB Laboratory and the Technion Material Engineering X-Ray Diffraction Laboratory for their assistance in this work.

ORCID iDs

Shlomi Bouscher  <https://orcid.org/0000-0002-0578-7493>
 Krishna Balasubramanian  <https://orcid.org/0000-0001-6307-7425>
 Alex Hayat  <https://orcid.org/0000-0002-6579-7431>

References

- [1] Bouscher S, Panna D and Hayat A 2017 Semiconductor–superconductor hybrid devices *J. Opt.* **19** 103003
- [2] Balasubramanian K, Xing X, Strugo N and Hayat A 2020 Thin-film-based integrated high-transition-temperature superconductor devices *Adv. Funct. Mater.* **30** 1807379
- [3] Tinkham M 1996 *Introduction to Superconductivity* 2nd edn (New York: McGraw-Hill)
- [4] Mou S S, Irie H, Asano Y, Akahane K, Kurosawa H, Nakajima H, Kumano H, Sasaki M and Suemune I 2015 Superconducting light-emitting diodes *IEEE J. Sel. Top. Quantum Electron.* **21** 7900111
- [5] Mou S S, Irie H, Asano Y, Akahane K, Nakajima H, Kumano H, Sasaki M, Murayama A and Suemune I 2015 Optical observation of superconducting density of states in luminescence spectra of InAs quantum dots *Phys. Rev. B* **92** 035308
- [6] Khoshnegar M and Majedi A H 2011 Entangled photon pair generation in hybrid superconductor–semiconductor quantum dot devices *Phys. Rev. B* **84** 104504
- [7] Sabag E, Bouscher S, Marjeh R and Hayat A 2017 Photonic Bell-state analysis based on semiconductor–superconductor structures *Phys. Rev. B* **95** 094503
- [8] Marjeh R, Sabag E and Hayat A 2016 Light amplification in semiconductor–superconductor structures *New J. Phys.* **18** 023019
- [9] Hayat A, Kee H Y, Burch K S and Steinberg A M 2014 Cooper-pair-based photon entanglement without isolated emitters *Phys. Rev. B* **89** 094508
- [10] Kastalsky A, Kleinsasser A W, Greene L H, Bhat R, Milliken F P and Harbison J P 1991 Observation of pair currents in superconductor–semiconductor contacts *Phys. Rev. Lett.* **67** 3026
- [11] Nguyen C, Kroemer H and Hu E L 1992 Anomalous Andreev conductance in InAs–AlSb quantum well structures with Nb electrodes *Phys. Rev. Lett.* **69** 2847
- [12] Nishino T, Hatano M, Hasegawa H, Kure T and Murai F 1990 Carrier reflection at the superconductor–semiconductor boundary observed using a coplanar-point-contact injector *Phys. Rev. B* **41** 7274(R)
- [13] Heslinga D R, Shafranjuk S E, van Kempen H and Klapwijk T M 1994 Observation of double-gap-edge Andreev reflection at Si/Nb interfaces by point-contact spectroscopy *Phys. Rev. B* **49** 10484
- [14] Panna D, Bouscher S, Balasubramanian K, Perepelook V, Cohen S, Ritter D and Hayat A 2018 Andreev reflection in a superconducting light-emitting diode *Nano Lett.* **18** 6764–9
- [15] Mott N F 1949 The basis of the electron theory of metals, with special reference to the transition metals *Proc. Phys. Soc. A* **62** 416
- [16] Basov D N and Timusk T 2005 Electrodynamics of high- T_c superconductors *Rev. Mod. Phys.* **77** 721–79
- [17] Lee P A, Nagaosa N and Wen X G 2006 Doping a Mott insulator: physics of high-temperature superconductivity *Rev. Mod. Phys.* **78** 17
- [18] Tranquada J M, Axe J D, Ichikawa N, Nakamura Y, Uchida S and Nachumi B 1996 Neutron-scattering study of stripe-phase order of holes and spins in $\text{La}_{1.48}\text{Nd}_{0.4}\text{Sr}_{0.12}\text{CuO}_4$ *Phys. Rev. B* **54** 7489
- [19] Timusk T and Statt B 1999 The pseudogap in high-temperature superconductors: an experimental survey *Rep. Prog. Phys.* **62** 61
- [20] Yuli O, Asulin I, Kalcheim Y, Koren G and Millo O 2009 Proximity-induced pseudogap: evidence for preformed pairs *Phys. Rev. Lett.* **103** 197003
- [21] Kashiwaya S and Tanaka Y 2000 Tunnelling effects on surface bound states in unconventional superconductors *Rep. Prog. Phys.* **63** 1641
- [22] Deutscher G 2005 Andreev–Saint-James reflections: a probe of cuprate superconductors *Rev. Mod. Phys.* **77** 109
- [23] Auerbach A and Altman E 2000 Andreev peaks and massive magnons in cuprate superconductor-normal-superconductor junctions *Phys. Rev. Lett.* **85** 3480
- [24] Lofwander T, Shumeiko V S and Wendin G 2001 Andreev bound states in high- T_c superconducting junctions *Supercond. Sci. Technol.* **14** R53
- [25] Milo O and Koren G 2016 What can Andreev bound states tell us about superconductors? *Phil. Trans. R. Soc. A* **376** 20140143
- [26] Carrington A, Manzano F, Prozorov R, Giannetta R W, Kameda N and Tamegai T 2001 Evidence for surface Andreev bound states in cuprate superconductors from penetration depth measurements *Phys. Rev. Lett.* **86** 1074
- [27] Asano Y, Tanaka Y and Kashiwaya S 2004 Phenomenological theory of zero-energy Andreev resonant states *Phys. Rev. B* **69** 134501
- [28] Alff L, Kleefisch S, Schoop U, Zittartz M, Kemen T, Bauch T, Marx A and Gross R 1998 Andreev bound states in high temperature superconductors *Eur. Phys. J. B* **5** 423–38
- [29] Chen D, Lin C, Maljuk A and Zhou F 2016 *Growth and Characterization of Bulk Superconductor Material* vol 243 (Berlin: Springer)
- [30] Russek S E, Sanders S C, Roshko A and Ekin J W 1994 Surface degradation of superconducting $\text{YBa}_2\text{Cu}_3\text{O}_{7-\delta}$ thin films *Appl. Phys. Lett.* **64** 3649

- [31] Zhou J-P, Loa R K, Savoy S M, Arendt M, Armstrong J, Yang D Y, Talvacchio J and McDevitt J T 1997 Environmental degradation properties of $\text{YBa}_2\text{Cu}_3\text{O}_{7-\delta}$ and $\text{Y}_{0.6}\text{Ca}_{0.4}\text{Ba}_{1.6}\text{La}_{0.4}\text{Cu}_3\text{O}_{7-\delta}$ thin film structures *Physica C* **273** 3–4
- [32] Sekimoto S, Watanabe C, Minami H, Yamamoto T, Kashiwagi T, Klemm R A and Kadowaki K 2013 Continuous 30 μW terahertz source by a high- T_c superconductor mesa structure *Appl. Phys. Lett.* **103** 182601
- [33] Colclough M S, Gough C E, Keene M, Muirhead C M, Thomas N, Abell J S and Sutton S 1987 Radio-frequency SQUID operation using a ceramic high-temperature superconductor *Nature* **328** 47–8
- [34] Perconte D *et al* 2018 Tunable Klein-like tunnelling of high-temperature superconducting pairs into graphene *Nat. Phys.* **14** 25–9
- [35] Leszczynski M, Teisseyre H, Suski T, Grzegory I, Bockowski M, Jun J and Porowski S 1996 Lattice parameters of gallium nitride *Appl. Phys. Lett.* **69** 73
- [36] Cheung J T, Gergis I, James M and DeWames R E 1992 Reproducible growth of high quality $\text{YBa}_2\text{Cu}_3\text{O}_{7-x}$ film on (100) MgO with a SrTiO_3 buffer layer by pulsed laser deposition *Appl. Phys. Lett.* **60** 3180
- [37] Low B L, Xu S Y, Ong C K, Wang X B and Shen Z X 1997 Substrate temperature dependence of the texture quality in YBCO thin films fabricated by on-axis pulsed-laser ablation *Supercond. Sci. Technol.* **10** 41
- [38] Panna D, Balasubramanian K, Bouscher S, Wang Y, Yu P, Chen X and Hayat A 2018 Nanoscale high- T_c YBCO/GaN super-Schottky diode *Sci. Rep.* **8** 5597
- [39] Tanaka Y and Kashiwaya S 1995 Theory of tunneling spectroscopy of d-wave superconductors *Phys. Rev. Lett.* **74** 3451
- [40] Yurtcan M T, Simsek Ö, Bayram Ö and Ertugrul M 2017 $\text{YBa}_2\text{Cu}_3\text{O}_{7-\delta}$ thin film growth on different substrates by pulsed laser deposition *Eastern Anatolian Journal of Science* **3** 1–7
- [41] Wu M K, Ashburn J R, Torng C J, Hor P H, Meng R L, Gao L, Huang Z J, Wang Y Q and Chu C W 1987 Superconductivity at 93 K in a new mixed-phase Y–Ba–Cu–O compound system at ambient pressure *Phys. Rev. Lett.* **58** 908
- [42] Blonder G E, Tinkham M and Klapwijk T M 1982 Transition from metallic to tunneling regimes in superconducting microconstrictions: excess current, charge imbalance and supercurrent conversion *Phys. Rev. B* **25** 4515
- [43] De Gennes P G 2018 *Superconductivity of Metals and Alloys* (Boca Raton, FL: CRC Press)
- [44] Cren T, Roditchev D, Sacks W, Klein J, Moussy J-B, Deville-Cavellin C and Laguës M 2000 Influence of disorder on the local density of states in high- T_c superconducting thin films *Phys. Rev. Lett.* **84** 147